Electronic Supplementary Information for

Thermodynamic and structural aspects of the aqueous uranium(IV) system – hydrolysis vs. sulfate complexation

Susanne Lehmann,[a] Harald Foerstendorf,[a] Thomas Zimmermann,[a,b] Michael Patzschke,[a] Frank Bok,[a] Vinzenz Brendler,[a] Thorsten Stumpf [a] and Robin Steudtner*[a]

a. Helmholtz-Zentrum Dresden-Rossendorf, Institute of Resource Ecology, Bautzner Landstr. 400, 01328 Dresden, Germany. E-mail: r.steudtner@hzdr.de

b. Dresden University of Applied Sciences, Fakultät Landbau / Umwelt / Chemie, Friedrich-List-Platz 1, 01069 Dresden.

Content

1 Residual U(VI) after electrochemical reduction

We employed LFS to quantify the unreduced amount of U(VI) in our stock solutions according to Opel et al. 2007.[1] Therefore, a serial dilution of U(VI) in 1 mol L^{-1} $HClO_4$ was measured as reference. At this low pH value UO_2^{2+} is the only expected U(VI) species in solution. The luminescence intensity of U(VI) in aqueous solution is proportional to its concentration. Thus, the maximum luminescence intensity at 510 nm of the serial dilution shows a linear behavior (Figure SI 1). The initial uranium U(VI) concentration for the electrochemical reduction was 10^{-2} mol L^{-1}. An aliquot of the stock solutions was diluted to 10^{-4} mol L^{-1} preliminary to LFS measurements. The measured U(VI) luminescence intensities (open symbols) after reduction ranged around 10^{-7} mol L^{-1}. Hence, the residual U(VI) concentration is calculated to be lower than 1% of the initial concentration.

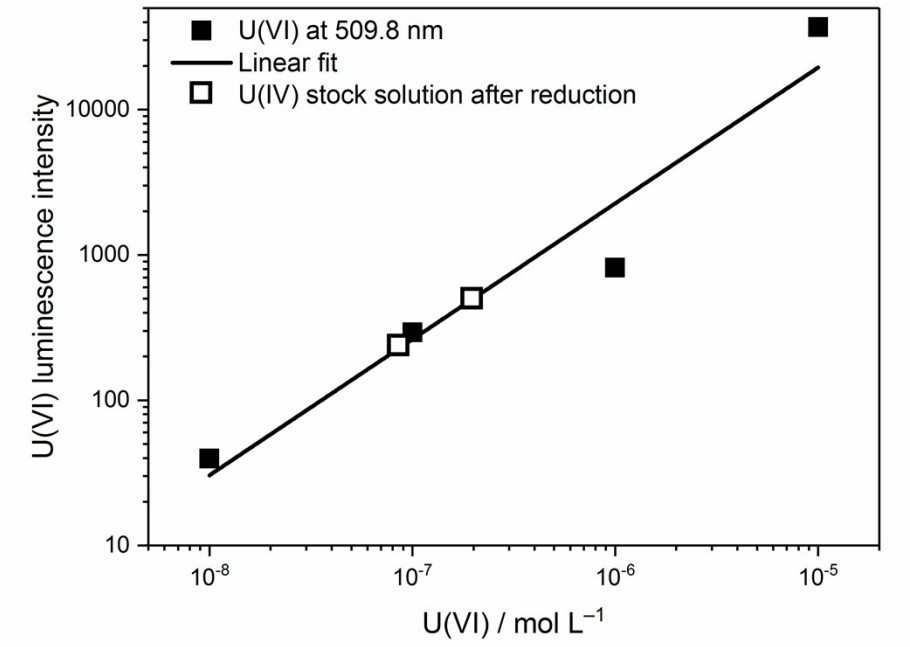

Figure SI 1: Luminescence intensity of U(IV) stock solutions excited at 266 nm in comparison to reference spectra of U(VI) at 509.8 nm.

2 Thermodynamic parameters used for calculations

Table SI 1: SIT coefficients for the system $U^{4+}/UO_2^{2+}/H^+/Na/Cl^-/ClO_4^-/SO_4^{2-}$ with associated uncertainties.

Interaction coefficient	Value	Reference	Remark
$\varepsilon(U^{4+},Cl^-)$	0.36 ± 0.01	[2]	Estimation
$\varepsilon(U^{4+},ClO_4^-)$	0.76 ± 0.06	[3]	Estimated in [4], an alternative value would be 0.84 ± 0.06, see remark (J) for table B-4 in [3]
$\varepsilon(USO_4^{2+},Cl^-)$	0.14 ± 0.1	p.w.	Estimated from the correlation given in [5]
$\varepsilon(USO_4^{2+},ClO_4^-)$	0.3 ± 0.1	[3]	Estimated in [4]
$\varepsilon(UO_2^{2+},Cl^-)$	0.21 ± 0.02	[3]	Taken from [6] but considered to be too low, an alternative value would be 0.46 ± 0.03, see remark (x) for table B-4 in [3]
$\varepsilon(UO_2^{2+},ClO_4^-)$	0.46 ± 0.03	[3]	
$\varepsilon(H^+,Cl^-)$	0.12 ± 0.01	[3]	
$\varepsilon(H^+,ClO_4^-)$	0.14 ± 0.02	[3]	
$\varepsilon(Na^+,Cl^-)$	0.03 ± 0.01	[3]	
$\varepsilon(Na^+,ClO_4^-)$	0.01 ± 0.02	[3]	
$\varepsilon(Na^+, SO_4^{2-})$	-0.12 ± 0.06	[3]	
$\varepsilon(Na^+, HSO_4^-)$	-0.01 ± 0.02	[3]	

The following SIT ion-ion-interaction coefficients are not available from literature: $\varepsilon(U^{4+}, SO_4^{2-})$, $\varepsilon(USO_4^{2+},SO_4^{2-})$, $\varepsilon(UO_2^{2+}, SO_4^{2-})$, and $\varepsilon(H^+, SO_4^{2-})$. Applying the SIT approach[6], the activity coefficient of the species j (taking part in the reaction) interacting with species k of opposite charge is expressed as:

$$log_{10}\gamma_j = -z_j^2 D + \sum_k \varepsilon(j;k) m_k \quad (1)$$

where z_j represents the charge of species j, $\varepsilon_{(j;k)}$ is the ion-ion-interaction coefficient between species j and k, m_k is the molality of species k, and D the Debye-Hückel term:

$$D = \frac{A\sqrt{I_m}}{1 + Ba_i\sqrt{I_m}} \quad (2)$$

In the Debye-Hückel term D, A is the Debye-Hückel constant being 0.509 $kg^{1/2}$ $mol^{-1/2}$ at 25 °C. The (empirical) constant Ba_i was chosen as 1.5 $kg^{1/2}$ $mol^{-1/2}$ for all temperatures up to 80 °C, as recommended by [7].

Inspecting equation (1) reveals that the first three missing interaction coefficients would be multiplied by the concentration of free sulfate, with a maximum of 10^{-4} mol L^{-1} at pH 2 (and lower values at all pH values below that, see Figure SI 2 for the respective sulfate speciation at low pH) and consequently not significantly affect the activity coefficient of U(IV). In case of $\varepsilon(H^+, SO_4^{2-})$, the same holds for the proton activity. When looking on the opposite, i.e. the sulfate activity coefficient, the first three missing interaction coefficients would be multiplied by the concentration of free tetravalent uranium, again a rather small value not exceeding 10^{-4} mol L^{-1} and thus being negligible. The only remaining problem would be the sulfate activity influenced by the proton concentration. Here (and of course also for the cases already discussed above), however, one should keep in mind that for each ion pair the respective interactions are formally identical to direct chemical reactions. And a split between the direct chemical reaction and the ion-ion-interaction is neither feasible nor realistic. Thus, an assignment to just one type of interaction (here: formation of the distinct species HSO_4^{2-}) should suffice.

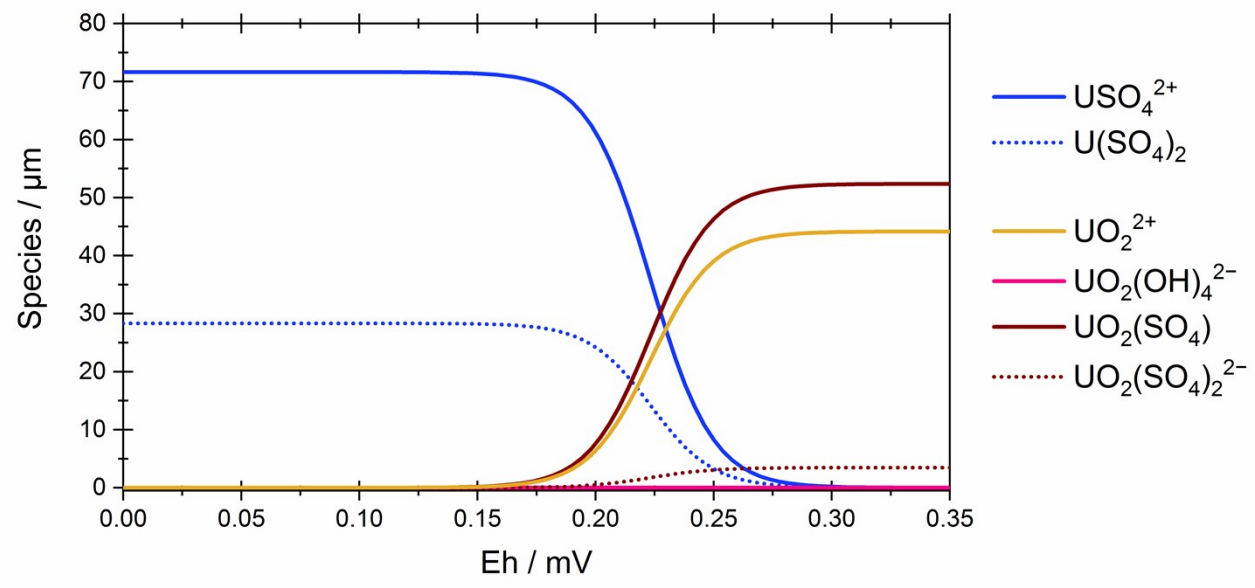

Figure SI 2: Eh dependent species distribution of 100 µmol L^{-1} [U] and 10 mmol L^{-1} [SO_4^{2-}] at I = 0.15 mol L^{-1} Na/HClO4 and pH 2.

Table SI 2: Binary Pitzer coefficients for the system $U^{4+}/UO_2^{2+}/H^+/ Na^+/Cl^-/ClO_4^-/SO_4^{2-}$

Cation i	Anion k	$\alpha^{(1)}$	$\alpha^{(2)}$	$\beta^{(0)}$	$\beta^{(1)}$	$\beta^{(2)}$	C^{Φ}	Reference
U^{4+}	Cl^-	2	0	1.27	13.5	0	0	8 a)
UOH^{3+}	Cl^-	2	0	0.6	5.9	0	0	8 a)
$U(OH)_2^{2+}$	Cl^-	2	0	0.23	1.93	0	0	8 a)
$U(OH)_3^+$	Cl^-	2	0	0.08	0.39	0	0	8 a)
$U(OH)_4(aq)$	Cl^-			$\lambda = 0 \pm 0.1$				8 b)
Na^+	$U(OH)_4(aq)$			$\lambda = 0 \pm 0.1$				8 b)
USO_4^{2+}	Cl^-	2	0	1.64	0	0	−0.2635	9
$U(SO_4)_2(aq)$	Cl^-			$\lambda = 0.29 \pm 0.1$				9

a) Based on conversion of SIT coefficients: better correlation of activity coefficients calculated with SIT and Pitzer parameters by simultaneous fit of $\beta^{(0)}_{ik}$ and $\beta^{(1)}_{ik}$ than by methods of [10], C^{Φ} and ternary parameters unknown (set to be zero); may lead to wrong activity coefficients with increasing ionic strength: parameter set is suitable only for chloride concentration < 0.5 mol L^{-1}.

b) Estimated according to Pitzer parameters of analogous species.

Table SI 3: Comparison of stability constants for U(IV) and U(VI) aqueous 1:1 complexes from NEA[3].

Ligand	Log K for U(IV)	Log K for U(VI)
OH^-	13.46 ± 0.06	8.75 ± 0.24
F^-	9.42 ± 0.51	5.16 ± 0.06
Cl^-	1.72 ± 0.13	0.17 ± 0.02
SO_4^{2-}	6.58 ± 0.19	3.15 ± 0.02
NO_3^-	1.47 ± 0.13	0.3 ± 0.15

3 Scoping experiments on U(IV) hydrolysis

Due to its high charge density and its high acidity as strong Lewis acid U(IV) is a very hard cation which tends to hydrolysis and precipitation.[11] Since precipitations would lead to clogging of LWCC during UV/vis measurements on the one hand and used thermodynamic models assume entire uranium to be in solution on the other hand, experimental conditions excluding precipitations were chosen by assessment of preliminary experiments with 1 $\mathrm{mmol\ L^{-1}}$ U(IV) in 0.2 $\mathrm{mol\ L^{-1}}$ $HClO_4/NaClO_4$ at various pH adjusted by coulometric titration.

An increase of particles in solution results in a baseline increase of UV/Vis absorption spectra due to scattering as shown in Figure SI 3, left. Until pH 1.84 no increase was observed. At pH 2.12 the baseline increase is already obvious. The determination of number of particles in solution by Dynamic Light Scattering (DLS) shows a fast increase at pH higher than 2 with first particles already occurring at pH 1.92 (Figure SI 3, middle). These findings have been confirmed by ultrafiltration. The Uranium concentration in 10 kDa ultrafiltrates is constant until pH 2. At pH higher than 2 the uranium concentration in solution decreases due to particle formation (Figure SI 3, right). These scoping results have been considered for experimental set up. Therefore, all speciation experiments were performed at pH values less than or equal to 2.

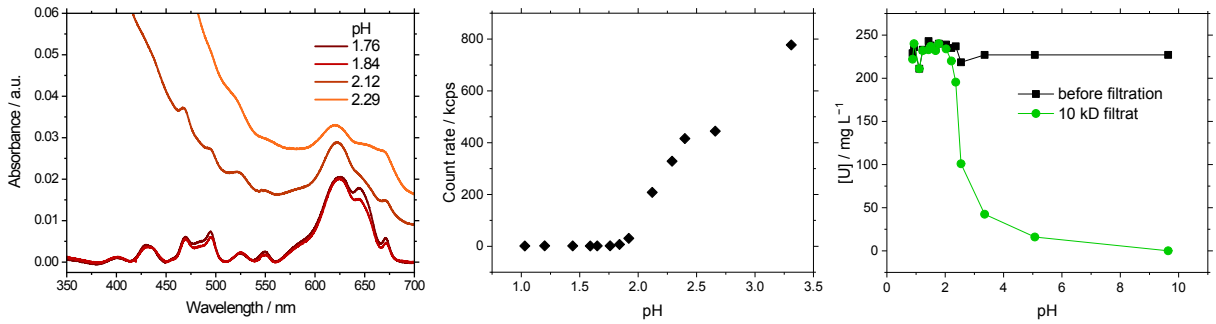

Figure SI 3: 1 $\mathrm{mmol\ L^{-1}}$ U(IV) in 0.2 $\mathrm{mol\ L^{-1}}$ $HClO_4/NaClO_4$ at various pH (coulometric titration). Left: UV/vis spectra measured in 1 cm cuvette illustrating the effect of increasing particle sizes on the baselines. Middle: Scattered light intensities measured by DLS showing increase of particles in solution. Right: Uranium concentration in 10 kDa ultrafiltrates of 1 $\mathrm{mmol\ L^{-1}}$ U(IV) in 0.2 $\mathrm{mol\ L^{-1}}$ $HClO_4/NaClO_4$ at various pH.

4 Additional UV/Vis absorption spectra

Overview of series 3 and 4 data sets in the range of 400-700 nm used as input data for HypSpec analysis at different pH.

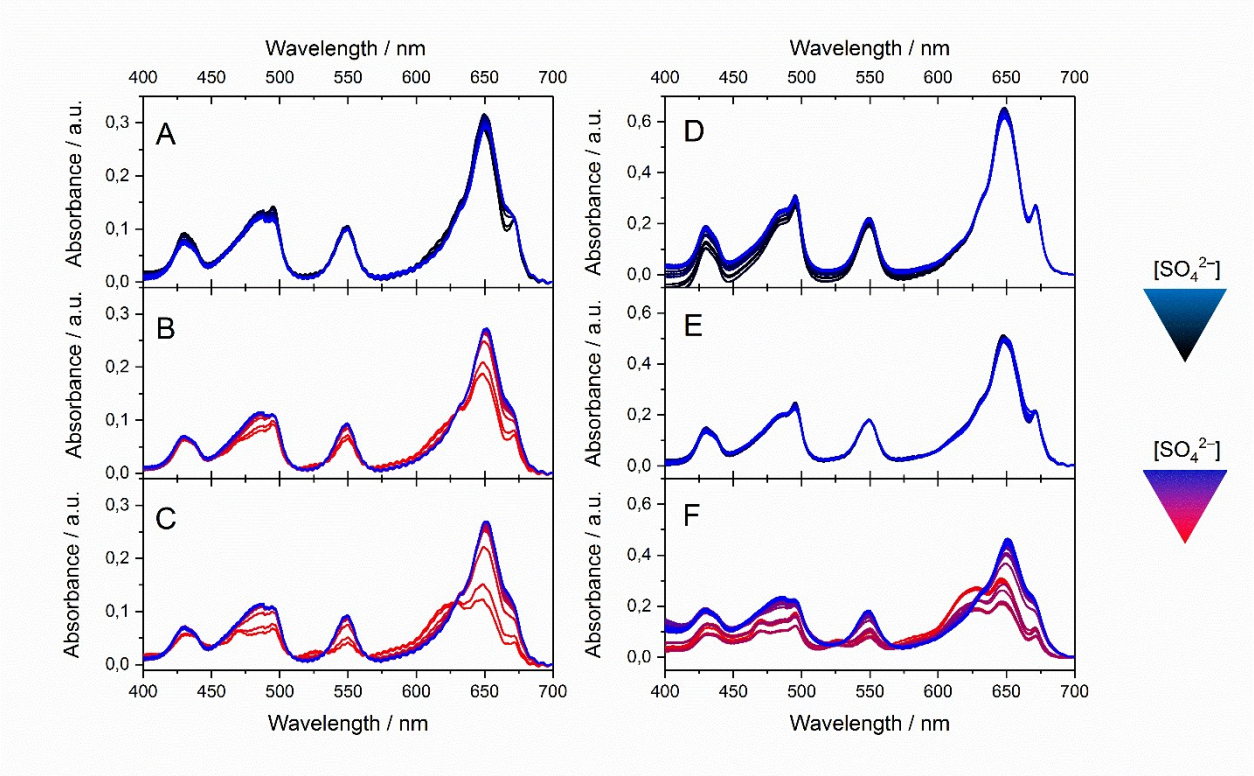

Figure SI 4: UV/vis data sets of sample series 3 at *I* = 0.15 $\mathrm{mol\ L^{-1}}$ at pH 1 (A), 1.5 (B) and 2 (C) and sample series 4 at *I* = 1.2 $\mathrm{mol\ L^{-1}}$, pH 0 (E), 1 (D) and 2 (F).

5 Speciation calculations

Speciation diagrams of series 3 and 4 were calculated twice: based on thermodynamic data from the NEA TDB and with stability constants derived from our UV/vis study. Both thermodynamic calculations are in good agreement with each other.

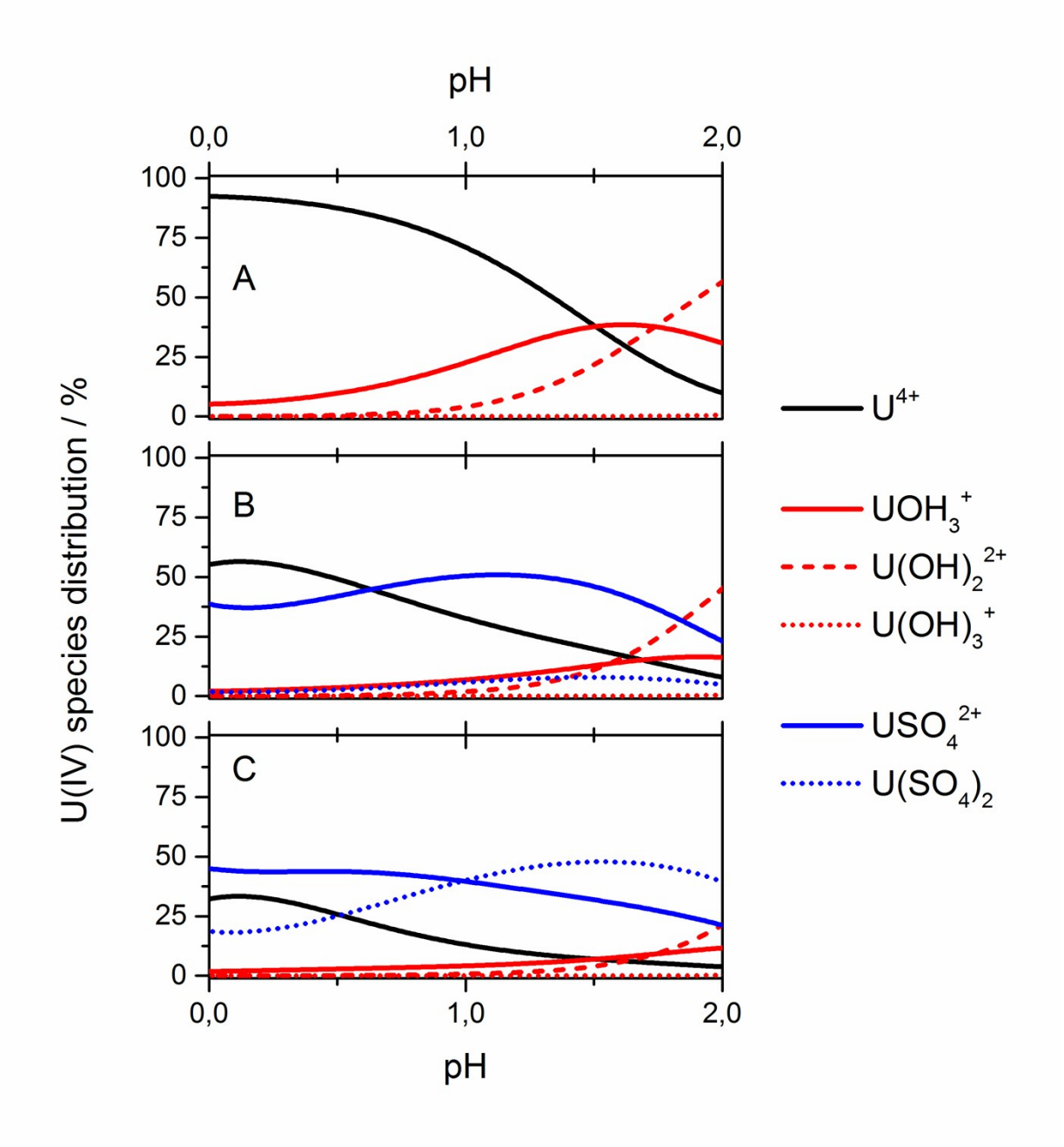

Figure SI 5: Speciation calculations of 100 µmol L^{-1} [U], at Eh = 0 mV and I = 1.2 mol L^{-1} Na/$HClO_4$ at pH 0 to 2. A) without sulfate B) with 1 mmol L^{-1} [SO_4^{2-}] using Data of NEA DTB C) with 1 mmol L^{-1} [SO_4^{2-}] using log ß determined in this work.

6 Consideration of vibrational modes, molecule symmetry and decomposition of IR spectra

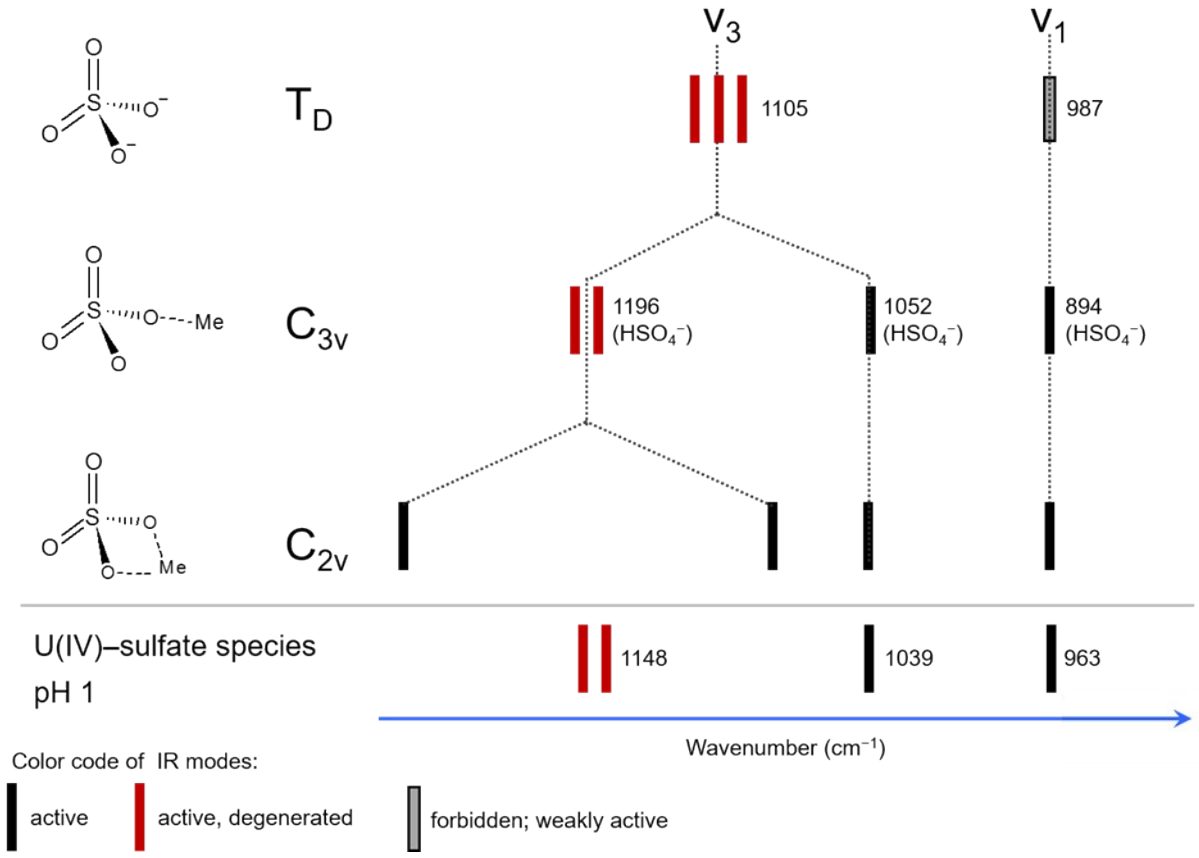

Figure SI 6: Correlation of vibrational modes observable in IR spectra and molecule symmetry of sulfate ions in different coordination modes. Note that the triply degenerated v_3 mode splits into two or three modes upon lowering the symmetry from T_D to C_{3v} or C_{2v}, respectively. In case of C_{3v} the split modes are denoted as antisymmetric ($v_{3,as}$) and symmetric ($v_{3,s}$) modes (from left to right). Values are given in cm^{-1}.

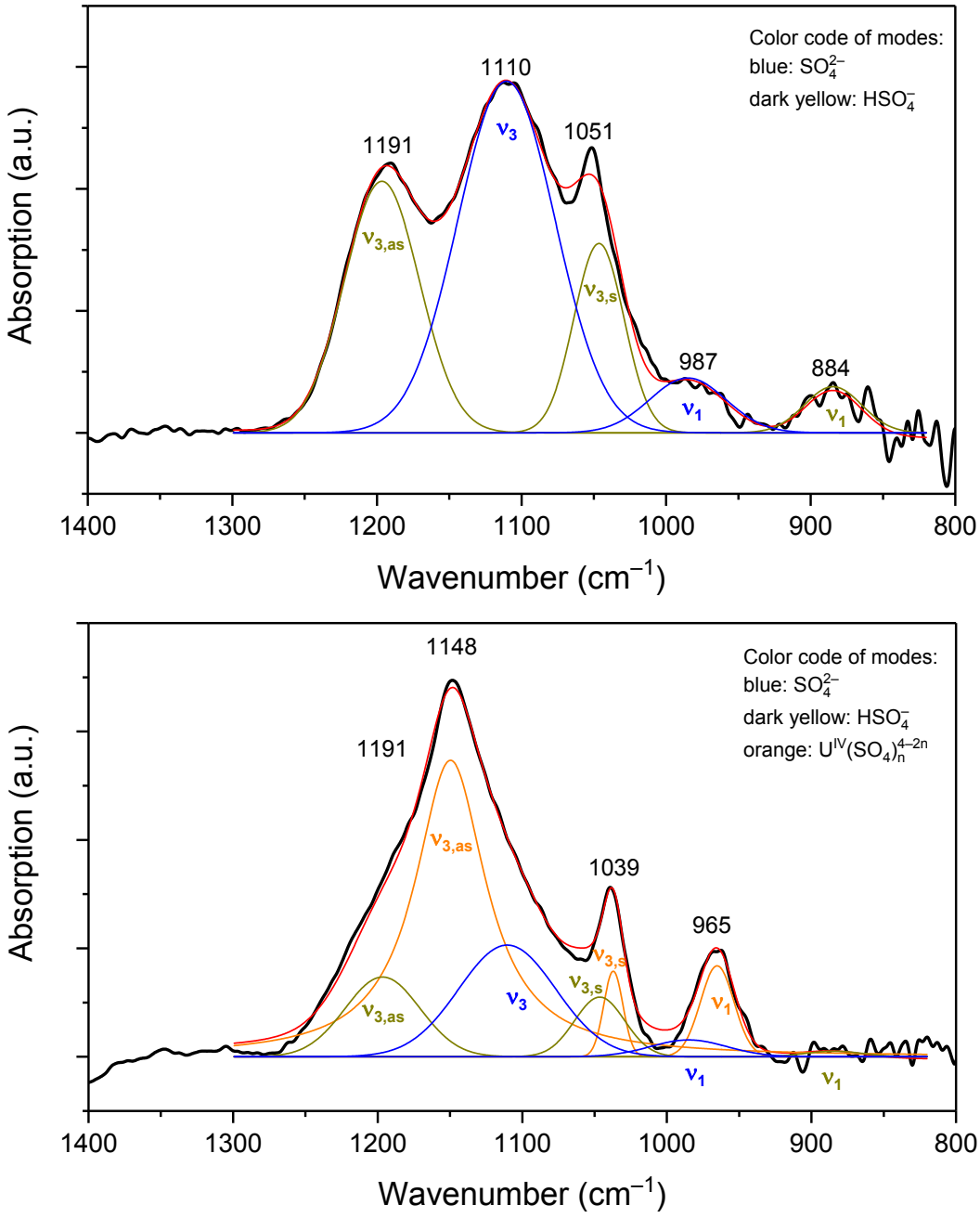

Figure SI 7: Spectral decomposition after second-derivative analysis and fitting of spectra of aqueous sulfate (pH 1, top) and of the corresponding U^{4+}-sulfate solution (below) in the frequency region 1300−825 cm^{-1}. For the fitting of the latter spectrum, the presence of uncoordinated sulfate was considered. Values are given in cm^{-1}.

7 USO_4^{2+} structure calculations with DFT and xTB

Starting from small clusters to build a first solvation shell around USO_4^{2+} was not successful. Following this approach would lead to the wrong conclusions entirely. Figure SI 8 shows the optimized structure of a cluster with 18 surrounding water molecules. For this kind of "clusters" mono- and bidentate structures could be found. The bidentate structure in Figure SI 8 fitted the experimental IR spectrum better than the monodentate structure (see Figure SI 9). This would have led to entirely wrong conclusions! The structures with 18 water molecules arose suspicion, as the number of water molecules connected to each sulfate oxygen was different. Therefore the alternative approach of starting with a big cluster, pre-optimizing the sulfate containing structure with xTB and then performing DFT optimizations, was chosen. The structure of the resulting water-sulfate cluster is shown in Figure SI 10. IR spectra of a pure water cluster containing 100 water molecules and of 100 water molecule cluster with one sulfate ion can be found in Figure Figure SI 11. Comparing the sulfate IR with experiment shows the right number of signals (three sharp signals around 1100 cm^{-1} and a diffuse signal around 900 cm^{-1}) this water cluster had no imaginary frequencies and it was therefore chosen as the starting point for the uranium-sulfate-water clusters. Starting from this cluster the uranium ions was added and the sulfate slightly rotated to create mono, bi and tridentate binding between the uranium ion and the sulfate ion. Optimization of these structures invariably led to monodentate binding motifs. Figure SI 12 shows a comparison between two such structures (C1 and C2 as discussed in the main text of the article) Figure SI 13 shows the vibrational mode that differs between C1 and C2.

Full optimization with DFT for the sulfate containing water clusters was tried. The number of cycles needed was very large, due to the flexibility of the cluster, the optimization was stopped when the energy changes were very low. At this point the forces on some water molecules were still rather high and therefore the calculated IR spectra were not used for comparison with experiment.

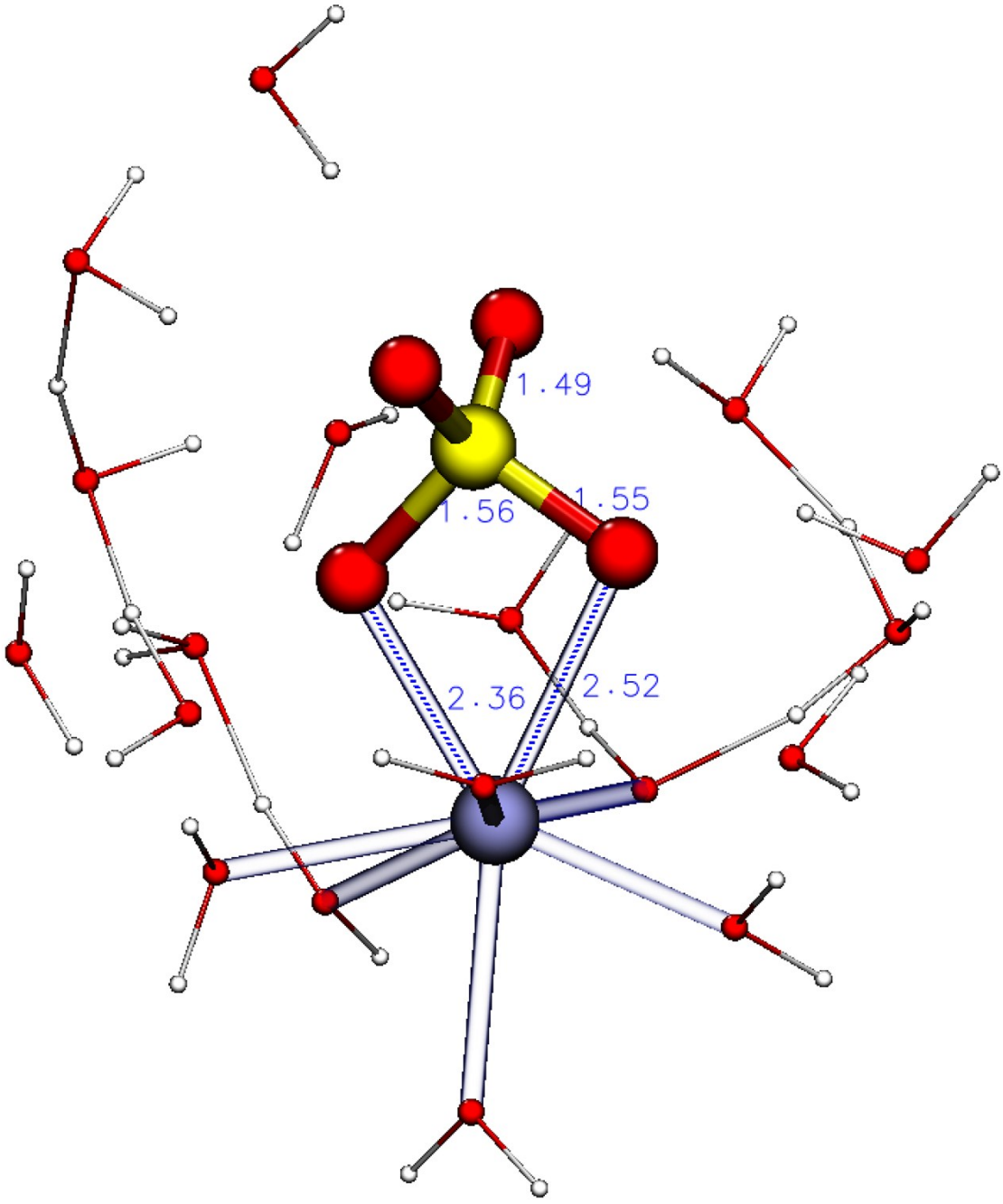

Figure SI 8: Optimized structure of a cluster containing 18 water molecules and 1 sulfate ion. The sorrounding extra water molecules are rendered much slimmer in order to improve the clearness of the picture

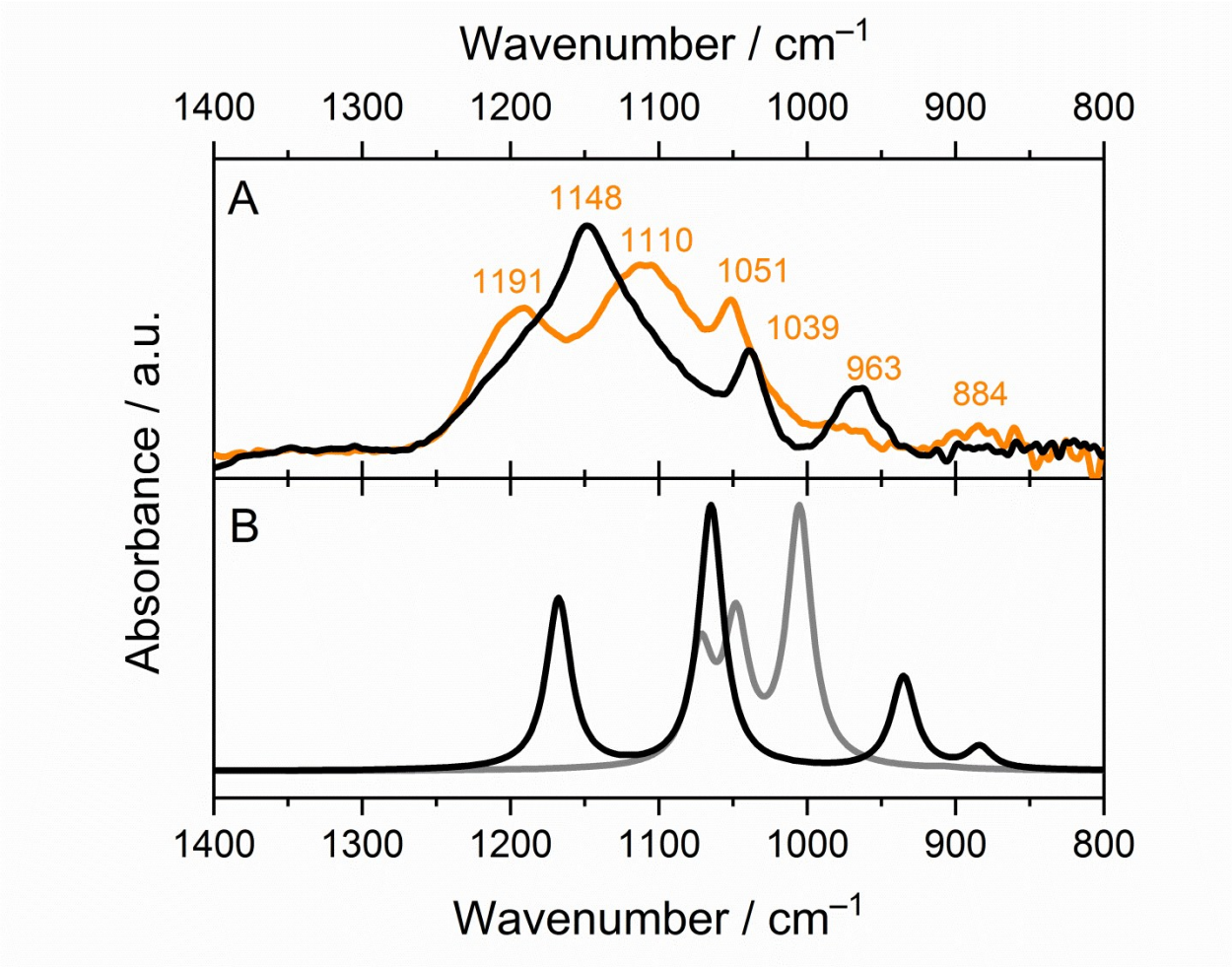

Figure SI 9: A) IR spectra of aqueous solution of sulfate (orange trace) and the corresponding U(IV) species (black trace). [Sulfate] = 1 mmol L^{-1}; [U] = 2 mmol L^{-1}; pH 1. B) Calculated IR spectra for the sulfate ion in an U(IV) sulfate complex with 18 water molecules. The grey line is for a monodentate complex, the black line is for the bidentate complex.

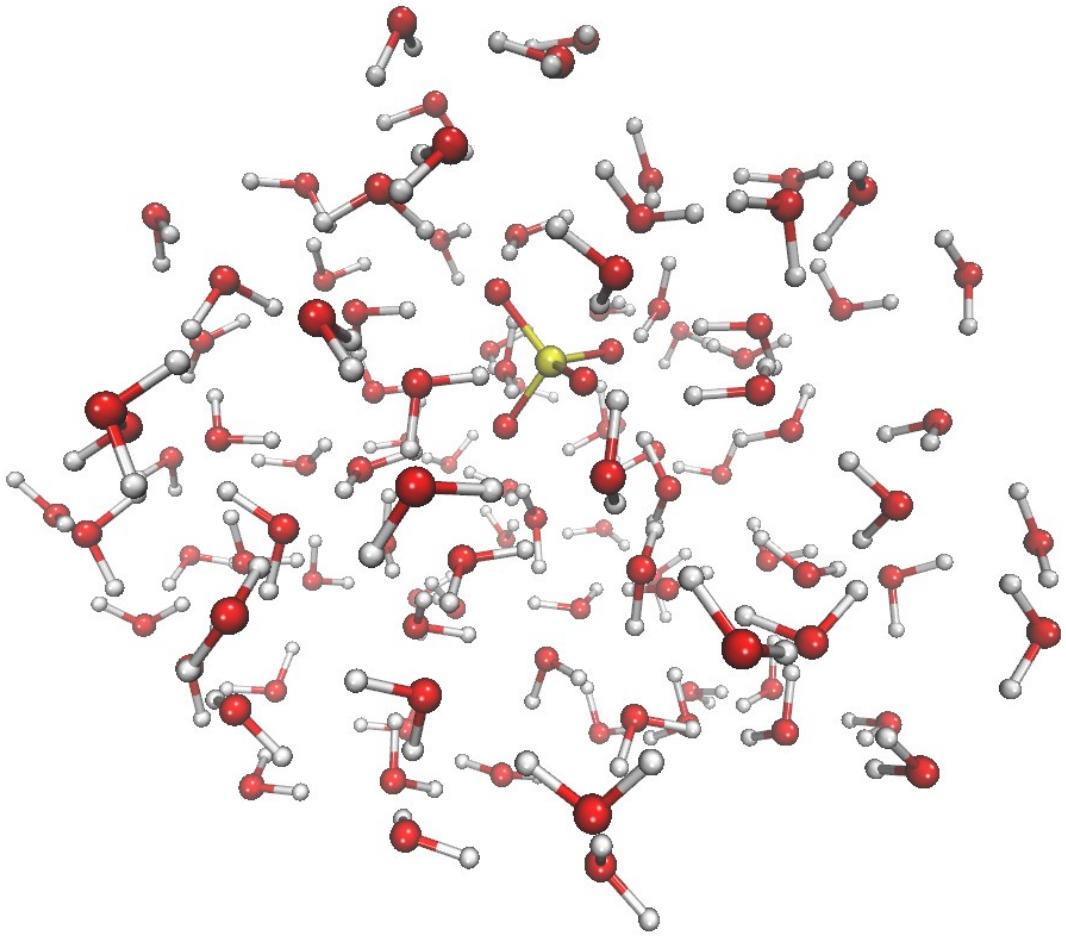

Figure SI 10: Structure of a cluster containing 100 water molecules and 1 sulfate ion. Optimized with tight-binding method.

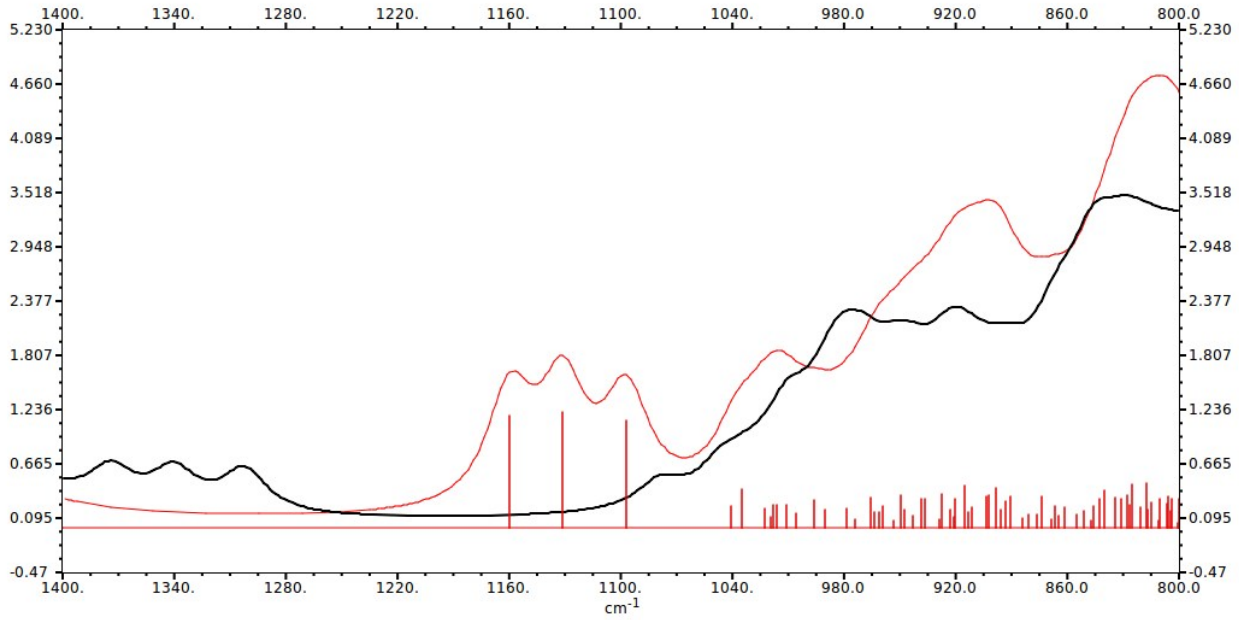

Figure SI 11: Calculated IR spectrum of a cluster consisting of 100 water molecules (black line) and IR spectrum of a cluster containing 100 water molecules and one sulfate ion (red line).

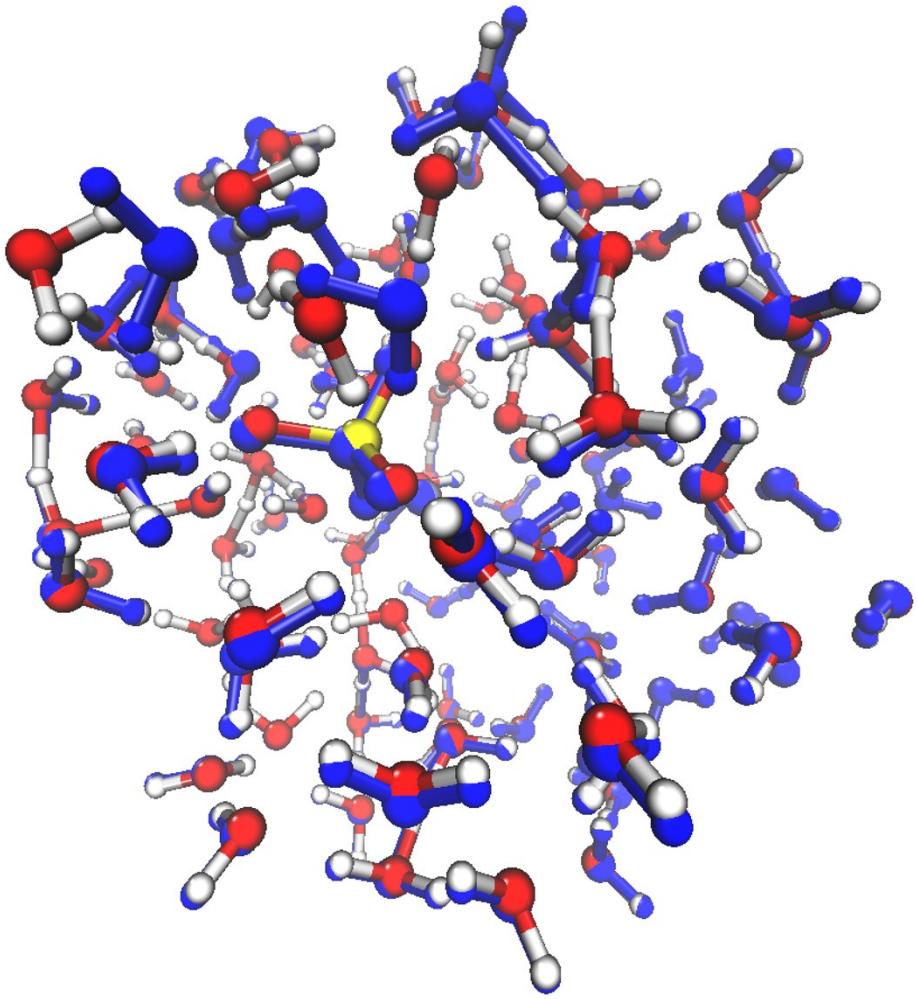

Figure SI 12: Two structures for uranium sulfate surrounded by 100 water molecules. Structure C1 is given in colors (oxygen red, sulfur yellow, hydrogen white, uranium steel blue). The structure of C2 is overlaid colored in blue only.

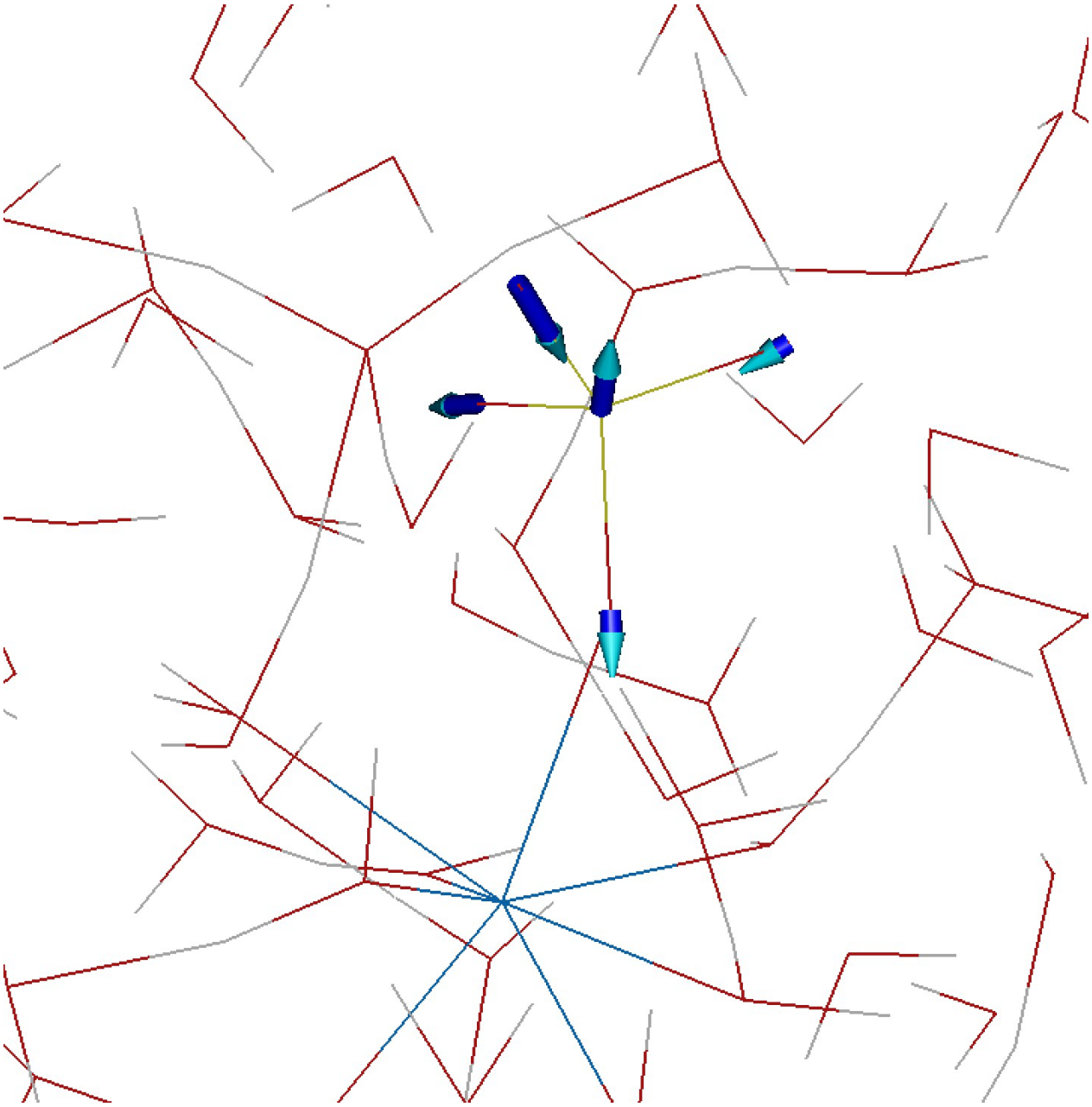

Figure SI 13 Vibrational mode affected by the structural differences between C1 and C2.

8 References

1. K. Opel, S. Weiss, S. Hubener, H. Zanker and G. Bernhard, *Radiochim Acta*, 2007, **95**, 143-149.
2. V. Neck and J. I. Kim, *Radiochim Acta*, 2001, **89**, 1-16.
3. R. Guillaumont, T. Fanghänel, J. Fuger, I. Grenthe, V. Neck, D. A. Palmer and M. H. Rand, *Update on the chemical thermodynamics of uranium, neptunium, plutonium, americium and technetium*, Elsevier, Amsterdam, 2003.
4. I. Grenthe, J. Fuger, R. J. M. Konings, R. J. Lemire, A. B. Müller, C. Nguyen-Trung and H. Wanner, *Chemical Thermodynamics of Uranium, OECD/NEA Data Bank*, Elsevier, Amsterdam, 1992.
5. V. Neck, M. Altmaier and T. Fanghanel, *Radiochim Acta*, 2006, **94**, 501-507.
6. L. Ciavatta, *Ann Chim*, 1980, **70**, 551-567.
7. R. J. Lemire, U. Berner, C. Musikas, D. A. Palmer, P. Taylor and O. Tochiyama, *Chemical Thermodynamics of Iron: Part I*, OECD Nuclear Energy Agency, Paris, 2013.
8. V. Neck, T. Fanghänel, V. Metz and B. Kienzler, *Kenntnisstand zur aquatischen Chemie und der thermodynamischen Datenbasis von Actiniden und Technetium. Abschlussbericht zum BfS-Projekt „Erstellung eines Nahfeldmodells von Gebinden hochradioaktiver Abfälle im Salzstock Gorleben: geochemisch fundierter Quellterm für HAW-Glas, abgebrannte Brennelemente und Zement*, FZK-INE, Karlsruhe, 2001.
9. D. Rai, L. Rao, H. Weger, A. R. Felmy and G. R. Choppin, *Thermodynamic data for predicting concentrations of Th(IV), U(IV), Np(IV), and Pu(IV) in geologic environments*, Pacific Northwest National Laboratory, Richland, 1999.
10. A. Plyasunov, T. Fanghanel and I. Grenthe, *Acta Chem Scand*, 1998, **52**, 250-260.
11. K. E. Knope and L. Soderholm, *Chem Rev*, 2013, **113**, 944-994.